The even pattern of xylan substitution is critical for interaction with cellulose in plant cell walls

Nicholas J. Grantham[1], Joel Wurman-Rodrich[1], Oliver M. Terrett[1], Jan J. Lyczakowski[1], Katherine Stott[1], Dinu Iuga[2], Thomas J. Simmons[1], Mylene Durand-Tardif[3], Steven. P. Brown[2], Ray Dupree[2], Marta Busse-Wicher[1], Paul Dupree[1*]

[1]Department of Biochemistry, University of Cambridge, Tennis Court Road, Cambridge, CB2 1QW, UK

[2]Department of Physics, University of Warwick, Coventry, CV4 7AL

[3]Institut Jean-Pierre Bourgin, UMR 1318, INRA AgroParisTech CNRS, Université Paris-Saclay, 78026 Versailles Cedex, France

*author for correspondence. Email : p.dupree@bioc.cam.ac.uk

Xylan and cellulose are abundant polysaccharides in vascular plants and essential for secondary cell wall strength. Acetate or glucuronic acid decorations are exclusively found on even-numbered residues in most of the xylan polymer. It has been proposed that this specific positioning of the decorations might permit docking of xylan onto the hydrophilic face of a cellulose microfibril[1–3]. Consequently, xylan adopts a flattened ribbon-like twofold helical screw conformation when bound to cellulose in the cell wall[4]. Here we show that ESKIMO1/XOAT1/TBL29, a xylan-specific O-acetyltransferase, is necessary for generation of the even pattern of acetyl esters on xylan. The reduced acetylation in the *esk1* mutant deregulates the position-specific activity of the xylan glucuronosyltransferase GUX1, and so the evenly-spaced pattern of glucuronic acid on the xylan is lost. Solid-state NMR of intact cell walls shows that, without the patterned xylan decorations, xylan does not interact normally with cellulose fibrils. We conclude that the even pattern of xylan substitutions seen across vascular plants therefore enables the interaction of xylan with hydrophilic faces of cellulose fibrils, and is essential for development of normal plant secondary cell walls.

Xylan is the principal hemicellulose in many plant secondary cell walls, and like cellulose is one of the most abundant polysaccharides on Earth[5,6]. It is thought that xylan hydrogen bonds with cellulose and may be crosslinked to lignin, forming a strong yet flexible composite material[7]. Despite the importance of the molecular architecture of plant cell walls for their material properties and digestibility, we are

just beginning to understand some aspects of cellulose microfibril structure and the molecular nature of the interactions of xylan with cellulose[3,4,8–10].

Xylan is a linear polymer of β-(1,4) linked D-xylosyl (X) residues. Xylan backbone decoration is ubiquitous in vascular plants, but the types of substitution vary. The most common substitutions are glucuronosyl (U) or 4-*O*-methylglucuronosyl (U^{Me}), arabinosyl (Ara) and acetyl (Ac) groups[11]. In solution, the molecule is flexible and forms a threefold helical screw[2,12]. However, we have recently shown using solid-state Nuclear Magnetic Resonance (NMR) that, upon association with cellulose in the cell wall, xylan adopts a twofold helical screw conformation with alternate xylosyl residues orientated 180° relative to each other[4]. Cellulose microfibrils have surfaces that are relatively hydrophobic, and also relatively hydrophilic surfaces that can hydrogen bond with water[8]. It is unknown whether xylan binds to the hydrophobic, hydrophilic, or both faces of cellulose fibrils[4,13]. Random backbone decorations would sterically impede xylan binding in a twofold screw conformation to the hydrophilic surfaces of the fibril, so this mode of binding has been considered unlikely. However, we recently found in many vascular plants from gymnosperms to eudicots[3], that many xylan molecules could be compatible with this cellulose binding mode, because decorations of $U^{[Me]}$, Ara and Ac are spaced with an even number of backbone X residues between them[1–3]. When the patterned xylan is flattened into the twofold screw ribbon, all the decorations become oriented along one side of the molecule. This might allow the xylan to dock and form hydrogen bonds with the hydrophilic surfaces of the cellulose microfibrils, forming semicrystalline 'xylanocellulose' fibrils, with the decoration facing away from the microfibril[1–4,14]. Without the substitutions restricted to alternate X residues, xylan may nevertheless be able to bind to cellulose on the hydrophobic face of microfibrils[2,15]. Despite the

indirect evidence supporting this model from the patterning of xylan and the molecular dynamics simulations, there are no direct experimental data to support the view that xylan binds to the hydrophilic surfaces of cellulose as proposed. It is not known whether the regular substitution patterns found in vascular plants are important for allowing the binding of xylan to cellulose. In this work, we show that modifying the pattern of substitutions prevents normal association with cellulose, providing experimental support for xylan binding largely to the hydrophilic surfaces of cellulose.

The presence of the patterns of xylan substitutions indicates that the biosynthetic machinery is finely regulated to generate precise molecular structures, yet we do not understand how the substitution pattern arises. Two glucuronosyltransferases, GUX1 and GUX2 add α-GlcA (U) decorations onto the 2-OH of around 12% of the X residues in xylan found in Arabidopsis secondary cell walls[16,17]. These U substitutions can subsequently be methylated to U^{Me} by methyltransferase enzymes[18]. GUX1 adds U groups to most of the xylan backbone invariably with an even number of backbone residues between decorations. In contrast, GUX2 adds tightly clustered U decorations with no such even spacing. Both types of U substitution patterns are present within the same molecules[1]. These enzymes show preferences in placing U on different positions of short xylan oligosaccharides *in vitro*[19], but it is unknown how GUX1 appears to achieve the remarkable task of placing U up to 20 X backbone residues apart, solely on even-numbered X residues[1].

Acetylation is the most abundant xylan decoration in eudicot plants and gnetophytes[3,11]. These acetyl esters are thought to prevent the xylan from

precipitating and may provide a hydrophobic surface for interaction with lignin[20,21]. In Arabidopsis, every second X residue is acetylated on the 2-OH, 3-OH or both 2 and 3-OH[2,22]. Most of the $U^{[Me]}$ decorations occur on the same X residues as the Ac, i.e. in phase with the acetylation pattern[2,22,23]. The four Reduced Wall Acetylation (*RWA)1-4* genes in Arabidopsis encode putative Ac-CoA transporters, and so are thought to supply Ac precursors to the Golgi acetyltransferases. In the *rwa1rwa3rwa4* and *rwa1rwa2rwa3* triple mutants, in which one functional RWA protein remains, xylan acetylation is reduced by 20-30%[24]. Xylan acetylation also requires the action of Trichome Birefringence Like (TBL) family proteins[25]. The ESKIMO1/XOAT1/TBL29 (ESK1) enzyme has been identified as a xylan-specific *O*-acetyltransferase[26] responsible for adding 50-60% of all xylan acetyl groups[25]. The *eskimo1* (*esk1*) mutant is dwarfed and shows collapsed xylem vessels, indicating that acetylation is important for xylan function and cell wall strength, although it is not clear why this is the case. A suppressor mutation, *kaktus* (*kak*), rescues the growth phenotype of the *esk1* mutant through increasing xylem vessel lumen area and partially restoring water conductivity, but does not restore acetylation of the xylan chain or wall strength[27].

To investigate the distribution of residual xylan Ac in the *rwa* and *esk1* mutants, xylan in delignified cell wall alcohol-insoluble residue (AIR) was hydrolysed with a GH10 xylanase. This enzymatic cleavage of xylan is restricted by Ac and $U^{[Me]}$ decorations, and yields some products with even length, such as X_4Ac_2, diagnostic of the acetylation pattern[2]. The MALDI-ToF mass spectra of the hydrolysed xylan showed minor differences in digestion products between WT and the *rwa* mutants, but *esk1* xylan was more extensively digested and the X_4Ac_2 product was not seen (Figure S1). Therefore, xylan from *esk1*, like *rwa* xylan, has reduced acetylation, but

in contrast to the *rwa* mutants, the even pattern of acetylation is not detected in the *esk1* mutant.

Reduction of xylan acetylation leads to increased $U^{[Me]}$ substitution of xylan, suggesting a link between acetylation and $U^{[Me]}$ substitution[28]. As expected, all the reduced acetylation mutants showed increased frequency of $U^{[Me]}$ decorations (Supplementary Figure 2). Next, the xylan $U^{[Me]}$ substitution patterns in the *rwa* and *esk1* mutants were determined and compared to WT patterns. Deacetylated WT and mutant xylan was hydrolysed with glucuronoxylanase GH30, which cleaves the xylan backbone one residue towards the reducing end from each glucuronosylated X residue, thus releasing oligosaccharides of a length corresponding to the distance between decorations[1,29]. Hydrolysis of the WT xylan produced dominant even degree of polymerisation (DP) oligosaccharides (Figure 1, $U^{[Me]}$X DP 6, 8, 10, 12). The *rwa* triple mutants showed similar dominant evenly spaced $U^{[Me]}$ patterns. The *rwa1rwa3rwa4* had a higher proportion of DP 6 oligosaccharides and lower proportion of DP 10, 12, consistent with a higher substitution frequency. However, the additional $U^{[Me]}$ in the xylan of *rwa* mutants does not disrupt the pattern. In contrast, the *esk1* mutant was devoid of any such even-spaced $U^{[Me]}$ patterning and relatively few oligosaccharides longer than DP12 were seen. Therefore, *rwa* and *esk1* are both acetylation-defective mutants showing increased $U^{[Me]}$ substitution. However, they show very different alterations to the patterning of the xylan decorations, indicating the ESK1 acetyltransferase is particularly important for generation of the patterned U substitutions of xylan.

To investigate whether the pattern of acetylation is also influenced by GUX enzyme activity, the acetylation in *gux1, gux2* and *gux1gux2* mutants was studied by MALDI-

ToF MS and solution NMR. As expected, the MALDI-ToF mass spectra of the GH10 xylanase hydrolysed xylan showed substantial differences in the proportions of oligosaccharides carrying U between WT and the *gux* mutants (Supplementary Figure 3). However, neutral oligosaccharides with even length diagnostic of the acetylation pattern, such as X_4Ac_2, were abundant in samples from WT and the *gux* mutants[2]. Intact acetylated xylan was analysed by two-dimensional $^{1}H–^{1}H$ nuclear Overhauser effect spectroscopy (NOESY) and ^{13}C HSQC NMR spectroscopy to investigate further the acetylation patterns in *esk1* and the *gux* mutants (Supplementary Figure 4). NOEs corresponding to unacetylated X adjacent to acetylated X residues, as previously identified[2] were observed in the WT, *gux1*, *gux2* and the *gux1gux2* mutants. However, they were largely absent from the *esk1* mutant acetylated xylan, further supporting the view that patterned acetylation requires ESK1, but is not substantially affected by GUX enzyme activity.

The increased glucuronosylation and the absence of the normal even-spaced pattern of $U^{[Me]}$ on xylan of *esk1* suggests that one or both GUX1 and GUX2 proteins change their U substitution pattern activity on the *esk1* poorly acetylated xylan. To investigate the contribution of each GUX enzyme in the *esk1* mutant, *esk1 gux* double and triple mutants were generated. The *esk1gux1* and *esk1gux2* double mutants grew slowly and were severely dwarfed, and the *esk1gux1gux2* triple mutant was extremely dwarfed (Figure 2). These severe phenotypes indicate there is an important role for both GUX1 and GUX2 in decorating xylan in *esk1*. To determine the contributions of each enzyme to the xylan decoration, the $U^{[Me]}$ frequency of the xylan from *esk1* and the *esk1gux* double mutants was determined (Figure 2B). Both the *esk1gux* double mutants showed a reduction in $U^{[Me]}$ frequency compared to the *esk1* single mutant, indicating that both enzymes contribute to the

xylan glucuronosylation in *esk1*. The relative contribution of each GUX enzyme to the total quantity of $U^{[Me]}$ was similar in *esk1* as it was in WT, with GUX1 providing quantitatively the most U decorations.

In WT plants, GUX1 places U decorations solely on even-spaced X residues, whereas GUX2 places decorations with an unpatterned distribution. To determine which of GUX1 or GUX2 produce the abnormal, unpatterned decorations in *esk1*, we analysed the xylan $U^{[Me]}$ decorations in the *esk1gux1* and *esk1gux2* double mutants by capillary and gel electrophoresis (Figure 2C, Supplementary Figure 5). The pattern of $U^{[Me]}$ decorations in the *esk1gux1* mutant was similar to that in the *gux1* mutant, consisting largely of DP 5, 6 and 7 oligosaccharides, although a few longer oligosaccharides could be detected. This indicates the GUX2 activity was not greatly altered in its positioning of the U substitutions. However, the pattern of $U^{[Me]}$ in the *esk1gux2* mutant, in contrast to the *gux2* mutant, did not show the even spacing normally catalysed by GUX1. Therefore, the specific manner in which GUX1 decorates xylan is profoundly altered in the *esk1* acetylation defective mutant.

According to the proposed model of xylan interaction with cellulose, the abnormal unpatterned xylan in *esk1* should be unable to interact with the hydrophilic face of cellulose, but could nevertheless interact with the hydrophobic face[2]. We studied whether changing the xylan substitution pattern alters xylan interactions with cellulose using solid-state NMR of unprocessed, never-dried stems. To obtain robust plants with substantial quantity of secondary cell walls for analysis, we grew *esk1* mutants suppressed in the growth phenotype by mutation of the *KAK* gene[27]. We confirmed that the patterns of xylan substitution in WT and the *esk1* mutant are not altered by the *kak* suppression (Supplementary Figure 6).

Xylan is induced to fold as a twofold screw through interaction with cellulose. This interaction and change in conformation leads to a change in the ^{13}C solid-state NMR chemical shift of xylosyl carbon 4 (C4) from the ^{13}C chemical shift of 77.4 ppm corresponding to the threefold screw found in solution to 82.2 ppm corresponding to the twofold screw[4]. A refocussed cross polarisation (CP) INADEQUATE spectrum of *esk1kak* showed that, in contrast to WT, the signal of xylan as a twofold screw was scarcely detectable in this xylan patterning mutant (Figure 3A). In contrast, threefold screw xylan was clearly observed in the mutant. As this CP-INADEQUATE emphasises the more rigid cell wall components, some of the xylan in *esk1* may therefore still interact with cellulose, but with a threefold screw conformation. The more mobile *esk1kak* cell wall components are shown in a direct polarisation INADEQUATE spectrum (Figure 3B). Unlike in the WT[4], relatively mobile threefold screw xylan is clearly seen in the *esk1kak* cell walls. Thus, the abnormal patterned xylan substitutions in the *esk1* mutant prevent normal interaction of xylan with cellulose and leads to an increase in unbound mobile xylan in the cell wall. The almost complete loss of the cellulose-bound two-fold screw xylan in the mutant suggests most of the xylan in WT plants binds to the hydrophilic face of cellulose in this xylan-substitution pattern-dependent manner.

Our findings indicate ESK1 is essential for generating the acetylation pattern. Additional TBLs and xylan acetylesterases may also be involved[30]. We now also know, since the *esk1* mutant shows disrupted patterns of U, that the glucuronosyltransferase GUX1 generates the even U pattern guided by the ESK1-dependent xylan acetylation. The sites for addition of U are in phase with (multiples of two residues from) patterned acetylated X residues (Figure 4). GUX1 may find gaps in the acetylation pattern, or compete with ESK1 and other TBLs for

substitution of appropriate X residues. Starvation of substrate in the *rwa* mutants may lead to an increase in frequency of these gaps, or a slight reduction in the ESK1/TBL activity, and results in an increase in GUX1 activity and patterned U substitutions. In the *esk1* mutant, larger regions of unacetylated xylan are available for GUX1 glucuronosyltransferase activity, and GUX1 is unable to maintain the correct U pattern without the acetylation guidance. There are several aspects of this model that are important areas of future investigation. How ESK1 is required for the Ac pattern generation, the role of other TBLs in acetylation, the subsequent transfer of additional acetate to X residues substituted by U, and the role of putative Golgi xylan acetylesterases remain unresolved[30].

There is a growing body of evidence that the patterned arrangement of xylan decorations is a common feature in all vascular plants[3]. Since the discovery of the xylan decoration pattern in Arabidopsis[1], it has been unclear what the importance of this is, if any, for xylan function. The pattern was suggested to be an essential feature allowing xylan to interact with hydrophilic surface of cellulose[2,3]. We have now shown that when the pattern of Ac and U is disrupted in *esk1*, the xylan does not bind in the twofold screw conformation to cellulose (Figure 3). This strongly supports the model of hydrogen bonding of the xylan with the hydrophilic surface of cellulose fibrils, as the pattern is essential for the docking onto this cellulose surface (Figure 4), but may not be essential for binding to the hydrophobic surfaces[2,3]. This work therefore provides critical evidence supporting this xylan-cellulose interaction hypothesis, and increases our understanding of the structure of xylanocellulose fibrils. It also demonstrates how such normal interactions may be disrupted, providing strategies to change plant cell walls for improved biorefining and

mechanical properties. Whether the loss of normal xylan binding to cellulose affects cellulose synthesis, fibril orientation or fibril aggregation remains to be investigated.

The binding of patterned xylan to the hydrophilic surfaces of cellulose fibrils in vascular plants could serve many roles. For instance, the modified surface of the xylanocellulose microfibril has greatly reduced H-bond donor capacity compared to the naked cellulose fibril surface. This, and the presence of acetyl esters, may alter the manner of fibril association with water, and could facilitate interactions with the hydrophobic lignin[2]. The lignocellulose assembly would be further strengthened if xylan is crosslinked to lignin via $U^{[Me]}$-lignin esters, as proposed[31]. Xylan binding to cellulose improves the mechanical properties of the cell wall, as shown by the fact that the *esk1* plants have collapsed vessels[32]. This coating of the fibrils may influence cellulose fibril bundling and interaction, perhaps preventing cellulose fibril co-crystallisation (aggregation). Pulp and paper manufacture, biofuel processing, and digestion of feed all involve removal of xylan from cellulose, and so discovery of plants in which xylan is not bound to cellulose may facilitate aspects of these processes[27,33,34]. This improved understanding of secondary cell wall architecture suggests novel strategies for preparation and application of biomaterials from plant cell walls.

EXPERIMENTAL PROCEDURES

Plant growth and cell wall preparation

Plants were *Arabidopsis thaliana* Columbia-0 ecotype. The *esk1* ethyl methanesulphonate induced point mutant (*esk1-1*)[35] was obtained from Henrik Scheller. T-DNA insertion mutations of ESKIMO1 (*esk1-5*) and KAKTUS (*kak-8*) were used for the NMR experiments[27]. Plants were grown in compost at 20°C, 100 µmol m^{-2} s^{-1} 16 h light / 8 h dark photoperiod 60% humidity and allowed five to six weeks to mature before harvesting, except the *esk1gux* double and triple mutants, which were grown aseptically in 0.5 x MS (Murashige and Skoog Basal Medium), 0.6% (w/v) agar for two weeks. They were then grown in magenta vessels containing the same media for three months prior to harvest. The basal five cm of fresh stems (entire stems for *esk1gux* double mutants) were harvested to make Alcohol Insoluble Residue (AIR) as previously described[1].

PACE and DASH

PACE (Polysaccharide Analysis by Carbohydrate gel Electrophoresis) and DASH (DNA sequencer Assisted Saccharide analysis in High throughput) was performed as previously described[1,36]. AIR was hydrolysed with *Bo*GH30[37], *Cj*GH10B or *Np*GH11A, kind gifts of Harry Gilbert, Newcastle. Deacetylation was carried out on dried samples by adding 20 µL of 4 M NaOH, incubating for 1 h and neutralising with 80 µL of 1 M HCl.

Mass Spectrometry

Matrix-assisted laser desorption/ionization time-of-flight (MALDI-ToF) mass spectrometry (MS) of xylanase digested samples was used to determine the spacing of Ac and $U^{[Me]}$ groups along the xylan backbone. For *Cj*GH10A hydrolysis, holocellulose was prepared from AIR by peracetic acid delignification, as described previously[2,38]. The holocellulose was then heat treated at 90 °C for 30 min in 100 mM ammonium acetate buffer, pH 5.5. The sample was centrifuged and the supernatant was discarded. Hydrolysis of the remaining pellet proceeded overnight at room temperature with xylanase *Cj*GH10A (approximately 1 μM). MALDI-ToF MS was performed using a 4700 Proteomics Analyser (Applied Biosystems, USA) as previously described[2,39]. The acetylated oligosaccharides in aqueous solution were mixed 1:1 (v/v) with 2,5-dihydroxybenzoic acid (DHB, Sigma-Aldrich) matrix (10 mg/mL DHB dissolved in 50% MeOH with 0.4 mg/mL Ammonium Sulphate ($(NH_4)_2SO_4$) to prevent the formation of disodiated adducts[40].

Solution NMR

Solution NMR of acetylated xylan (prepared by DMSO extraction as described for Mass Spectrometry) was carried out as described in[2]. The NMR data of *gux1gux2* acetylated xylan were reanalysed from [2].

Solid-State Nuclear Magnetic Resonance

MAS solid-state NMR experiments used ^{13}C enriched plants grown and labelled with $^{13}CO_2$ in a bespoke growth chamber according to Simmons et al[4]. Experiments were performed on a widebore Bruker (Karlsruhe, Germany) AVANCE III 850 MHz solid-state NMR spectrometer operating at 20 T, corresponding to ^{1}H and ^{13}C Larmor frequencies of 850.2 and 213.8 MHz, respectively. Experiments were conducted at

298 room temperature using a 3.2 mm low E field biosolids MAS probe at a MAS
299 frequency of 12.5 kHz ± 5 Hz. The ^{13}C chemical shift was determined using the
300 carbonyl peak at 177.8 ppm of L-alanine as an external reference with respect to
301 TMS. Two-dimensional double-quantum (DQ) correlation spectra were recorded
302 using the refocused INADEQUATE pulse sequence[41,42], which relies upon the use of
303 isotropic, scalar J coupling to obtain through-bond information regarding directly
304 coupled nuclei. Both ^{1}H to ^{13}C CP, with ramped ^{1}H amplitude and a contact time of 1
305 ms, and direct polarisation (to emphasise the mobile constituents) versions of the
306 experiment were used to produce the initial transverse magnetization. The ^{1}H 90°
307 pulse length was 3.5 µs and the ^{13}C 90° and 180° pulse lengths were 4.2 and 8.4 µs,
308 respectively, with a spin-echo delay of 2.24 ms. SPINAL-64 decoupling[43] at a ^{1}H
309 nutation frequency of 70 kHz during evolution and signal acquisition periods was
310 used throughout. The recycle delay was 1.9 s. The spectral width was 50 kHz in both
311 dimensions with the acquisition time in the indirect dimension (t_1) being 4.5 ms with
312 128 co-added transients for each slice in the CP experiment using the States method
313 for sign discrimination in F_1 and 5.0 ms with 96 co-added transients for each slice in
314 the direct polarisation experiment using the TPPI method for sign discrimination in
315 F_1. The data obtained were Fourier transformed into 2K (F_2) × 1K (F_1) points with EM
316 line broadening of 40 Hz in F_2 and squared sine bell in F_1. All spectra obtained were
317 processed and analysed using Bruker Topspin version 3.2.

318 **Author contributions**

319 NJG conducted most of the plant molecular genetic and biochemical experiments,
320 assisted by JWR and MBW. MDT provided *esk1kak* genetic material and supporting
321 information. The solid state NMR experiments were conducted by RD assisted by DI

using plants grown by TJS, OMT and JL. Solution NMR was conducted by KS and NJG. Data analysis was conducted by NJG, JWR, OMT, JL, KS, TJS, MBW, SPB, RD, PD. MBW, SPB, RD and PD supervised aspects of the project. The paper was written by NJG, MBW and PD with contributions from all authors.

Keywords

Arabidopsis thaliana, xylan, acetylation, glucuronosylation, cellulose interaction, ESKIMO1, acetyltransferase

Acknowledgements

This work was part supported by the Leverhulme Trust grant for the Centre for Natural Material Innovation. JWR, JJL and OMT are supported by studentships from Conicyt Chile and the Cambridge Trusts, the BBSRC Doctoral Training Partnership BB/J014540/1, and a BBSRC Novozymes iCASE award (BB/M015432/1) respectively. We thank Kris B Krogh for co-supervision of OMT. The UK 850 MHz solid-state NMR Facility used in this research was funded by EPSRC and BBSRC (Contract reference PR140003), as well as the University of Warwick including via part funding through Birmingham Science City Advanced Materials Projects 1 and 2 supported by Advantage West Midlands (AWM) and the European Regional Development Fund (ERDF).

FIGURES

Figure 1: $U^{[Me]}$ decoration patterns are disrupted in *esk1* but not *rwa* acetylation mutants. Xylan from WT, *rwa1rwa3rwa4*, *rwa1rwa2rwa3* and *esk1* mutants was hydrolysed with glucuronoxylanase GH30 and analysed by DASH capillary electrophoresis (DNA-sequencer-Assisted Saccharide analysis in High-throughput). (a) capillary electrophoresis traces and (b, c) quantification of oligosaccharides showing loss of the predominantly even pattern of $U^{[Me]}$ spacing in *esk1*. Values are means ± standard deviation (SD) of three independent biological replicates of basal stems from at least five plants, each replicate analysed by three independent hydrolyses. ns not statistically significant; * p≤0.05; ** p≤0.01; *** p≤0.001; by two-tailed t-test. Dagger, background peak.

Figure 2: Both GUX1 and GUX2 contribute to glucuronosylation in the *esk1* mutant, but GUX1 is deregulated in its patterning activity. (a) The *esk1* mutant is fertile but dwarfed to approximately 50% of wild type height[25]. In contrast, both the *esk1gux1* and the *esk1gux2* double mutants are sterile and severely dwarfed. The triple *esk1gux1gux2* mutant did not grow an inflorescence stem. Bars 1 cm. (b) Both GUX1 and GUX2 contribute to xylan glucuronosylation in the *esk1* mutant in similar proportions to WT background. $U^{[Me]}$ frequencies were measured by DASH capillary electrophoresis of GH11 xylanase hydrolysed xylan. Values are means ± standard deviation (SD) of three independent hydrolyses of a single biological replicate of five plants, and are representative of two independent experiments. * p≤0.05 in both replicates by two-tailed t-test. (c) DASH capillary electrophoresis analysis of GH30 glucuronoxylanase digested xylan indicates that *esk1gux2* double mutants show clear altered $U^{[Me]}$ patterning similar to the *esk1* mutant, indicating GUX1 is deregulated in *esk1*. Dagger, a primary cell wall xylan PUX_6 oligosaccharide[44].

Figure 3: Solid-state NMR of WT and *esk1kak* mutant cell walls shows that the unpatterned xylan does not bind to cellulose in the twofold helical screw conformation found in WT plants. (a) An overlay is shown of the carbohydrate regions of refocussed CP-INADEQUATE spectra of WT and the *esk1kak* mutant. The Double Quantum (DQ) shift is the sum of the Single Quantum shifts of two bonded (J-coupled) ^{13}C nuclei. Red labelling indicates xylan in the cellulose-bound, twofold screw conformation. The absence of the $Xn4^{2f}$-$Xn5^{2f}$ pair in *esk1kak* indicates twofold screw xylan bound to cellulose is reduced in the mutant. The green labelled xylan in the threefold conformation is substantially more abundant in the *esk1kak* mutant cell walls. (b) A refocussed direct polarisation INADEQUATE spectrum of the *esk1kak* mutant shows that the abnormal, relatively mobile, threefold screw xylan is found in the mutant cell walls. Spectra are representative of data from two independent biological replicates.

Figure 4: A model of xylan substitution pattern generation and its consequence for xylan interaction with cellulose. Xylan is first synthesised by the xylan synthase complex (XSC) in the Golgi apparatus. The pattern of xylan acetylation on alternate X residues requires the action of ESK1, and perhaps additional enzymes. Next, GUX1 places a U on even-spaced X residues directed by the pattern of Ac, leading to patterned xylan that is compatible with binding to the cellulose hydrophilic surface. GUX2 places a U without maintaining the pattern with other decorations, generating incompatible xylan. After initial acetylation and glucuronosylation, the xylan may be further modified by additional TBL acetyl transferases that place an Ac on the same X that is substituted by a U, and which may generate doubly acetylated X residues. The pattern of xylan acetylation may also be influenced by acetyl-xylan esterases[30]. In the *esk1* mutant (right), the absence of the acetylation catalysed by ESK1 results in GUX1 decorating the xylan with U at incorrect positions, and the defective xylan is incompatible with binding to cellulose hydrophilic surfaces.

References

1. Bromley, J. R. *et al.* GUX1 and GUX2 glucuronyltransferases decorate distinct domains of glucuronoxylan with different substitution patterns. *Plant J.* **74,** 423–434 (2013).
2. Busse-Wicher, M. *et al.* The pattern of xylan acetylation suggests xylan may interact with cellulose microfibrils as a twofold helical screw in the secondary plant cell wall of Arabidopsis thaliana. *Plant J.* **79,** 492–506 (2014).
3. Busse-Wicher, M. *et al.* Evolution of xylan substitution patterns in gymnosperms and angiosperms: implications for xylan interaction with cellulose. *Plant Physiol.* **171,** pp.00539.2016 (2016).
4. Simmons, T. J. *et al.* Folding of xylan onto cellulose fibrils in plant cell walls revealed by solid-state NMR. *Nat. Commun.* **7,** 13902 (2016).
5. Scheller, H. V. & Ulvskov, P. Hemicelluloses. *Annu. Rev. Plant Biol.* **61,** 263–289 (2010).
6. Kumar, M., Campbell, L. & Turner, S. Secondary cell walls: Biosynthesis and manipulation. *J. Exp. Bot.* **67,** 515–531 (2016).
7. Cosgrove, D. J. & Jarvis, M. C. Comparative structure and biomechanics of plant primary and secondary cell walls. *Front. Plant Sci.* **3,** 204 (2012).
8. Fernandes, A. N. *et al.* Nanostructure of cellulose microfibrils in spruce wood. *Proc. Natl. Acad. Sci.* **108,** E1195–E1203 (2011).
9. Thomas, L. H. *et al.* Diffraction evidence for the structure of cellulose microfibrils in bamboo, a model for grass and cereal celluloses. *BMC Plant Biol.* **15,** 153 (2015).

10. Wang, T. & Hong, M. Solid-state NMR investigations of cellulose structure and interactions with matrix polysaccharides in plant primary cell walls. *J. Exp. Bot.* **67,** 503–514 (2016).
11. Ebringerová, A. & Heinze, T. Xylan and xylan derivatives – biopolymers with valuable properties, 1. Naturally occurring xylans structures, isolation procedures and properties. *Macromol. Rapid Commun.* **21,** 542–556 (2000).
12. Nieduszynski, I. A. & Marchessault, R. H. Structure of β-D-(1→4′)Xylan Hydrate. *Biopolymers* **11,** 1335–1344 (1972).
13. Li, L., Pérré, P., Frank, X. & Mazeau, K. A coarse-grain force-field for xylan and its interaction with cellulose. *Carbohydr. Polym.* **127,** 438–450 (2015).
14. Pereira, C. S., Silveira, R. L., Dupree, P. & Skaf, M. S. Effects of Xylan Side-Chain Substitutions on Xylan-Cellulose Interactions and Implications for Thermal Pretreatment of Cellulosic Biomass. *Biomacromolecules* **18,** 1311–1321 (2017).
15. Kabel, M. A., De Waard, P., Schols, H. A. & Voragen, A. G. J. Location of O-acetyl substituents in xylo-oligosaccharides obtained from hydrothermally treated Eucalyptus wood. *Carbohydr. Res.* **338,** 69–77 (2003).
16. Mortimer, J. C. *et al.* Absence of branches from xylan in Arabidopsis gux mutants reveals potential for simplification of lignocellulosic biomass. *Proc. Natl. Acad. Sci.* **107,** 17409–17414 (2010).
17. Oikawa, A. *et al.* An integrative approach to the identification of arabidopsis and rice genes involved in xylan and secondary wall development. *PLoS One* **5,** e15481 (2010).
18. Urbanowicz, B. R. *et al.* 4-O-methylation of glucuronic acid in Arabidopsis glucuronoxylan is catalyzed by a domain of unknown function family 579

protein. *Proc. Natl. Acad. Sci.* **109,** 14253–14258 (2012).

19. Rennie, E. A. *et al.* Three Members of the Arabidopsis Glycosyltransferase Family 8 Are Xylan Glucuronosyltransferases. *Plant Physiol.* **159,** 1408–1417 (2012).

20. Pawar, P. M.-A., Koutaniemi, S., Tenkanen, M. & Mellerowicz, E. J. Acetylation of woody lignocellulose: significance and regulation. *Front. Plant Sci.* **4,** 118 (2013).

21. Busse-Wicher, M., Grantham, N. J., Lyczakowski, J. J., Nikolovski, N. & Dupree, P. Xylan decoration patterns and the plant secondary cell wall molecular architecture. *Biochem. Soc. Trans.* **44,** 74–78 (2016).

22. Chong, S. L. *et al.* O-Acetylation of glucuronoxylan in arabidopsis thaliana wild type and its change in xylan biosynthesis mutants. *Glycobiology* **24,** 494–506 (2014).

23. Koutaniemi, S. *et al.* Substituent-specific antibody against glucuronoxylan reveals close association of glucuronic acid and acetyl substituents and distinct labeling patterns in tree species. *Planta* **236,** 739–751 (2012).

24. Manabe, Y. *et al.* Reduced Wall Acetylation Proteins Play Vital and Distinct Roles in Cell Wall O-Acetylation in Arabidopsis. *Plant Physiol.* **163,** 1107–1117 (2013).

25. Xiong, G., Cheng, K. & Pauly, M. Xylan O-acetylation impacts xylem development and enzymatic recalcitrance as indicated by the arabidopsis mutant tbl29. *Mol. Plant* **6,** 1373–1375 (2013).

26. Urbanowicz, B. R., Peña, M. J., Moniz, H. A., Moremen, K. W. & York, W. S. Two Arabidopsis proteins synthesize acetylated xylan in vitro. *Plant J.* **80,** 197–206 (2014).

27. Bensussan, M. *et al.* Suppression of Dwarf and *irregular xylem* Phenotypes Generates Low-Acetylated Biomass Lines in Arabidopsis. *Plant Physiol.* **168,** 452–463 (2015).

28. Xiong, G., Dama, M. & Pauly, M. Glucuronic Acid Moieties on Xylan Are Functionally Equivalent to O-Acetyl-Substituents. *Mol. Plant* **8,** 1119–1121 (2015).

29. Vršanská, M., Kolenová, K., Puchart, V. & Biely, P. Mode of action of glycoside hydrolase family 5 glucuronoxylan xylanohydrolase from Erwinia chrysanthemi. *FEBS J.* **274,** 1666–1677 (2007).

30. Zhang, B. *et al.* Control of secondary cell wall patterning involves xylan deacetylation by a GDSL esterase. *Nat. Plants* **3,** 17017 (2017).

31. Das, N. N., Das, S. C. & Mukherjee, A. K. On the ester linkage between lignin and 4-O-methyl-d-glucurono-d-xylan in jute fiber (Corchorus capsularis). *Carbohydr. Res.* **127,** 345–348 (1984).

32. Lefebvre, V. *et al.* ESKIMO1 disruption in Arabidopsis alters vascular tissue and impairs water transport. *PLoS One* **6,** e16645 (2011).

33. Kabel, M. A., van den Borne, H., Vincken, J. P., Voragen, A. G. J. & Schols, H. A. Structural differences of xylans affect their interaction with cellulose. *Carbohydr. Polym.* **69,** 94–105 (2007).

34. Himmel, M. E. *Biomass Recalcitrance: Deconstructing the Plant Cell Wall for Bioenergy*. *Biomass Recalcitrance: Deconstructing the Plant Cell Wall for Bioenergy* (Blackwell Publishing Ltd., 2009). doi:10.1002/9781444305418

35. Xin, Z. & Browse, J. eskimo1 mutants of Arabidopsis are constitutively freezing-tolerant. *Proc. Natl. Acad. Sci.* **95,** 7799–7804 (1998).

36. Li, X. *et al.* Development and application of a high throughput carbohydrate

profiling technique for analyzing plant cell wall polysaccharides and carbohydrate active enzymes. *Biotechnol. Biofuels* **6,** 94 (2013).

37. Rogowski, A. *et al.* Glycan complexity dictates microbial resource allocation in the large intestine. *Nat. Commun.* **6,** 7481 (2015).

38. Gonçalves, V. M. F., Evtuguin, D. V. & Domingues, M. R. M. Structural characterization of the acetylated heteroxylan from the natural hybrid Paulownia elongata/Paulownia fortunei. *Carbohydr. Res.* **343,** 256–266 (2008).

39. Günl, M., Gille, S. & Pauly, M. OLIgo Mass Profiling (OLIMP) of Extracellular Polysaccharides. *J. Vis. Exp.* (2010). doi:10.3791/2046

40. Enebro, J. & Karlsson, S. Improved matrix-assisted laser desorption/ionisation time-of-flight mass spectrometry of carboxymethyl cellulose. *Rapid Commun. Mass Spectrom.* **20,** 3693–3698 (2006).

41. Lesage, A., Bardet, M. & Emsley, L. Through-bond carbon-carbon connectivities in disordered solids by NMR. *J. Am. Chem. Soc.* **121,** 10987–10993 (1999).

42. Fayon, F. *et al.* Through-space contributions to two-dimensional double-quantum J correlation NMR spectra of magic-angle-spinning solids. *J. Chem. Phys.* (2005). doi:10.1063/1.1898219

43. Fung, B. M., Khitrin, A. K. & Ermolaev, K. An improved broadband decoupling sequence for liquid crystals and solids. *J. Magn. Reson.* (2000). doi:Doi 10.1006/Jmre.1999.1896

44. Mortimer, J. C. *et al.* An unusual xylan in Arabidopsis primary cell walls is synthesised by GUX3, IRX9L, IRX10L and IRX14. *Plant J.* **83,** 413–426 (2015).

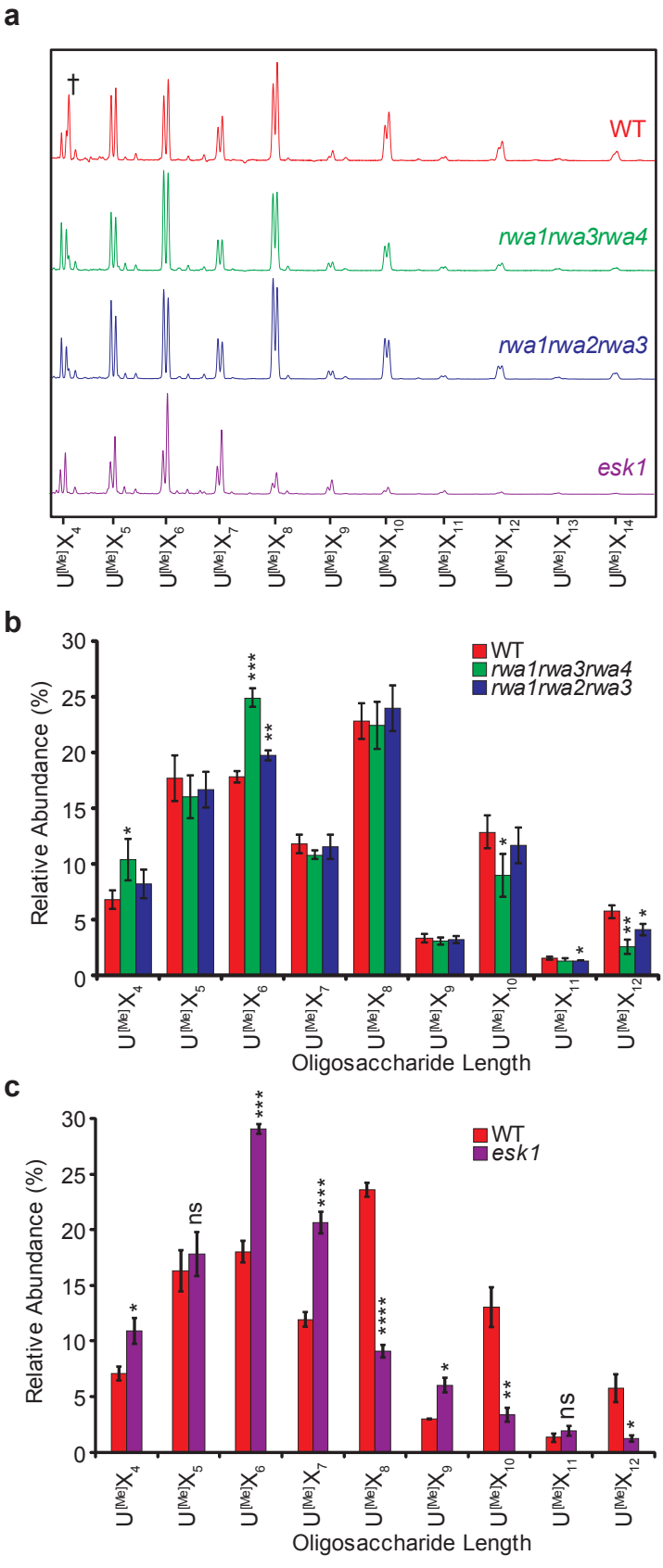
a
†
WT
rwa1rwa3rwa4
rwa1rwa2rwa3
esk1
U[Me]X4
U[Me]X5
U[Me]X6
U[Me]X7
U[Me]X8
U[Me]X9
U[Me]X10
U[Me]X11
U[Me]X12
U[Me]X13
U[Me]X14
b
WT
rwa1rwa3rwa4
rwa1rwa2rwa3
Relative Abundance (%)
Oligosaccharide Length
c
WT
esk1
Relative Abundance (%)
ns
Oligosaccharide Length

Figure 1

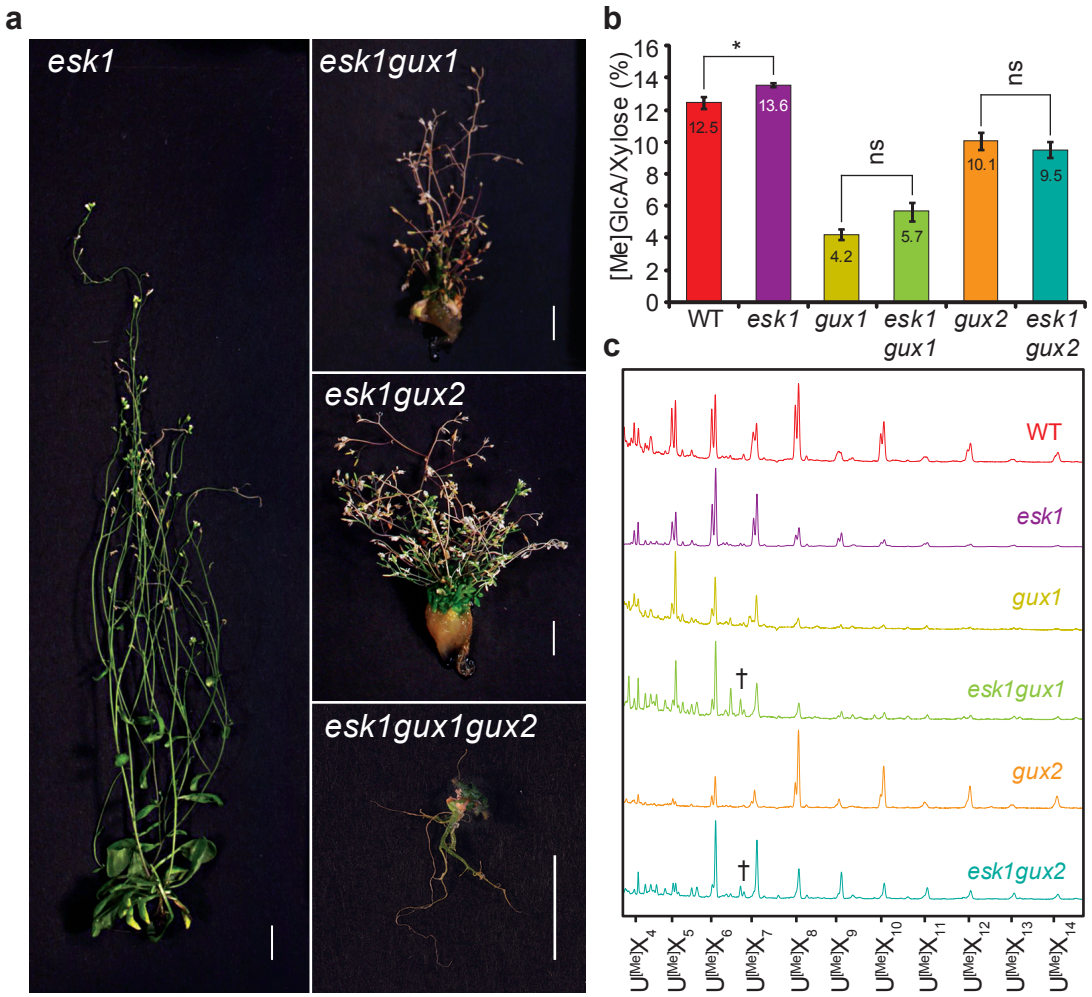
a
esk1
esk1gux1
esk1gux2
esk1gux1gux2
b
[Me]GlcA/Xylose (%)
16
14
12
10
8
6
4
2
0
*
ns
ns
12.5
13.6
4.2
5.7
10.1
9.5
WT
esk1
gux1
esk1 gux1
gux2
esk1 gux2
c
WT
esk1
gux1
esk1gux1
gux2
esk1gux2
†
†
U[Me]X4
U[Me]X5
U[Me]X6
U[Me]X7
U[Me]X8
U[Me]X9
U[Me]X10
U[Me]X11
U[Me]X12
U[Me]X13
U[Me]X14

Figure 2

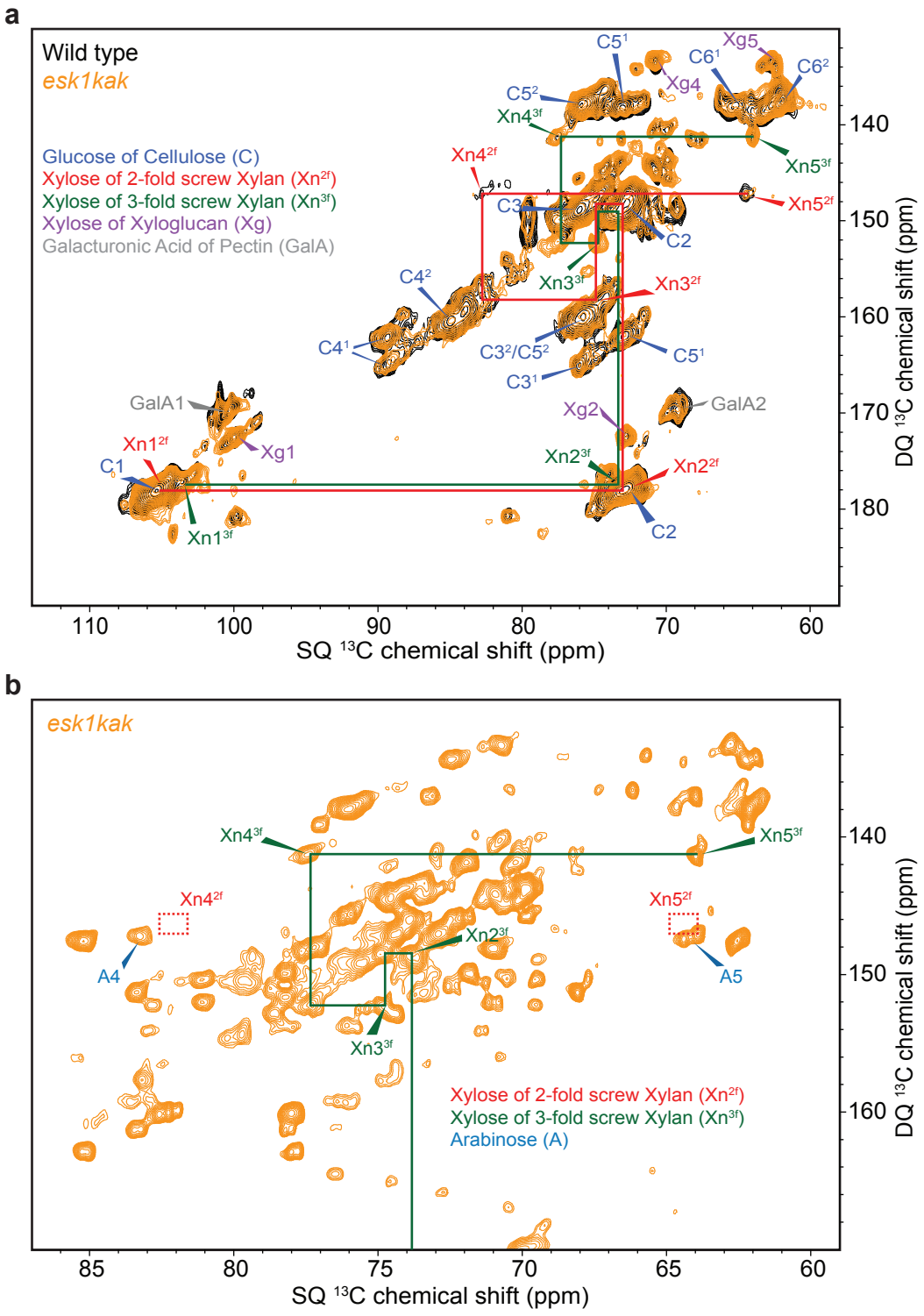
a
Wild type
esk1kak
Glucose of Cellulose (C)
Xylose of 2-fold screw Xylan (Xn2f)
Xylose of 3-fold screw Xylan (Xn3f)
Xylose of Xyloglucan (Xg)
Galacturonic Acid of Pectin (GalA)
C5¹
C6¹
Xg5
C6²
Xg4
C5²
Xn4³f
Xn4²f
Xn5³f
Xn5²f
C3
C2
C4²
Xn3³f
Xn3²f
C4¹
C3²/C5²
C5¹
C3¹
GalA1
Xg2
GalA2
Xn1²f
Xg1
C1
Xn2³f
Xn2²f
C2
Xn1³f
110
100
90
80
70
60
SQ ¹³C chemical shift (ppm)
140
150
160
170
180
DQ ¹³C chemical shift (ppm)
b
esk1kak
Xn4³f
Xn5³f
Xn4²f
Xn5²f
Xn2³f
A4
A5
Xn3³f
Xylose of 2-fold screw Xylan (Xn2f)
Xylose of 3-fold screw Xylan (Xn3f)
Arabinose (A)
85
80
75
70
65
60
SQ ¹³C chemical shift (ppm)
140
150
160
DQ ¹³C chemical shift (ppm)

Figure 3

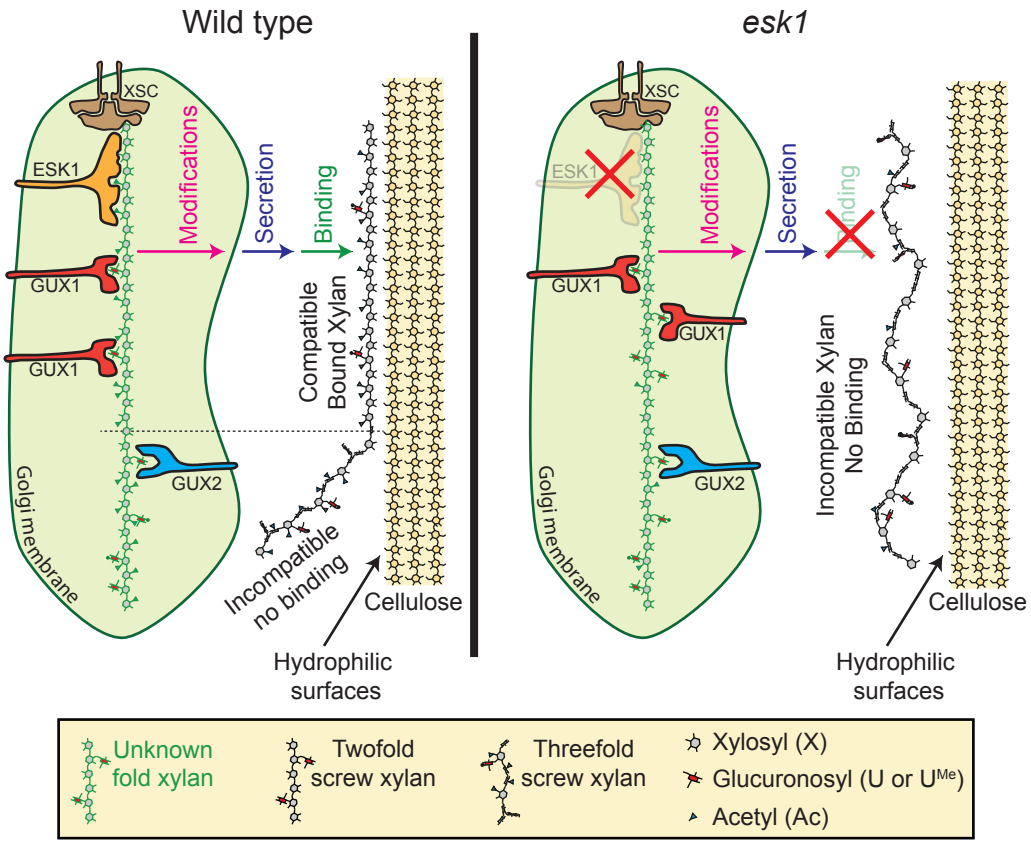
Wild type
esk1
XSC
ESK1
GUX1
GUX1
GUX2
Golgi membrane
Modifications
Secretion
Binding
Compatible
Bound Xylan
Incompatible
no binding
Cellulose
Hydrophilic
surfaces
XSC
ESK1
GUX1
GUX1
GUX2
Golgi membrane
Modifications
Secretion
Incompatible Xylan
No Binding
Cellulose
Hydrophilic
surfaces
Unknown
fold xylan
Twofold
screw xylan
Threefold
screw xylan
Xylosyl (X)
Glucuronosyl (U or U^Me)
Acetyl (Ac)

Figure 4